J|A|C|S
ARTICLES
Published on Web 07/07/2006

Mechanism of the Aerobic Oxidation of Alcohols by Palladium Complexes of N-Heterocyclic Carbenes

Robert J. Nielsen and William A. Goddard III*

Contribution from the Materials and Process Simulation Center, Beckman Institute (139-74), Division of Chemistry and Chemical Engineering, California Institute of Technology, Pasadena, California 91125

Received February 7, 2006; E-mail: wag@wag.caltech.edu

Abstract: Quantum mechanics (B3LYP density functional theory) combined with solvation (Poisson−Boltzmann polarizable continuum solvent model) was used to investigate six mechanisms for the aerobic oxidation of alcohols catalyzed by (NHC)Pd(carboxylate)$_2$(H_2O) complexes (NHC = 1,3-bis(2,6-diisopropylphenyl)imidazol-2-ylidene). Of these, we find that "reductive β-hydride elimination", in which the β-hydrogen of a palladium-bound alkoxide is transferred directly to the free oxygen of the bound carboxylate, provides the lowest-energy route and explains the published kinetic isotope effect, activation enthalpy, reaction orders, and dependence of rate on carboxylate pK_a. The traditional β-hydride elimination mechanism cannot be responsible for the experimentally observed kinetic parameters, which we find could result from the subsequent reductive elimination of acetic acid, which yields a slightly higher calculated activation barrier. Reversible β-hydride elimination may provide a mechanism for the racemization of chiral alcohols, which would undermine attempts at an enantioselective oxidation. Competition among these pathways can be influenced by changing the electronic properties of the carboxylate and substrate.

1. Introduction

Our motivation is to find a ligand system for palladium(II) to perform efficient oxidative kinetic resolutions of secondary alcohols. The chelating diamine (−)-sparteine (Figure 1) brings enantioselectivity to palladium-catalyzed aerobic oxidations of benzylic and allylic secondary alcohols, routinely fostering selectivity factors (k_R/k_S) over 20.[1−4] In chloroform, resolutions are efficient at ambient temperature and oxygen pressure. However, saturated substrates react slowly and are poorly resolved, and the antipode (+)-sparteine is not widely available. The ideal ligand would be easily synthesized in both enantiomers and expand the substrate scope offered currently by ((−)-sparteine)$PdCl_2$ protocols.[1,2,5,6]

Palladium dichloride complexes of chiral and achiral N-heterocyclic carbenes (NHC) were shown by the Sigman group to oxidize 1-phenylethanol enantioselectively when (−)-sparteine was present in solution to act as a chiral deprotonating agent.[7] A more efficient, though unselective, catalyst employs an NHC ligand on palladium diacetate (**0** in Figure 1) and has recently been described in detail.[8,9] Rates higher than those

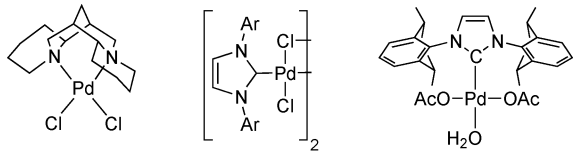

((-)-sparteine)$PdCl_2$ **0**

Figure 1. Some ligand systems for Pd-catalyzed alcohol oxidations.

afforded by the (−)-sparteine protocol were observed for both benzylic and saturated secondary alcohols. This allows a lower catalyst loading (Pd:substrate ratio of 1:200) than required by kinetic resolutions using ((−)-sparteine)$PdCl_2$ (1:20).

We chose to pursue the possibility of kinetic resolutions employing dissymmetric N-heterocyclic carbenes. Besides their favorable reactivity, NHCs provide great synthetic flexibility in their construction, and many C_1- and C_2-symmetric versions are already known.[10−14] The rate-limiting step of alcohol oxidations by ((−)-spartieine)$PdCl_2$ complexes is β-hydride elimination of a palladium hydride from a palladium-bound alkoxide. We found that enantioselectivities in that case could be calculated from the relative energies of diastereomeric β-hydride elimination transition states incorporating *R* or *S* substrates.[15] To use a similar approach to screen hypothesized

(1) Ferreira, E. M.; Stoltz, B. M. *J. Am. Chem. Soc.* **2001**, *123*, 7725.
(2) Jensen, D. R.; Pugsley, J. S.; Sigman, M. S. *J. Am. Chem. Soc.* **2001**, *123*, 7475.
(3) Ali, I. S.; Sudalai, A. *Tetrahedron Lett.* **2002**, *43*, 5435.
(4) Caspi, D. D.; Ebner, D. C.; Bagdanoff, J. T.; Stoltz, B. M. *Adv. Synth. Catal.* **2004**, *346*, 185.
(5) Bagdanoff, J. T.; Ferreira, E. M.; Stoltz, B. M. *Org. Lett.* **2003**, *5*, 835.
(6) Bagdanoff, J. T.; Stoltz, B. M. *Angew. Chem., Int. Ed.* **2004**, *43*, 353.
(7) Jensen, D. R.; Sigman, M. S. *Org. Lett.* **2003**, *5*, 63.
(8) Mueller, J. A.; Goller, C. P.; Sigman, M. S. *J. Am. Chem. Soc.* **2004**, *126*, 9724.
(9) Jensen, D. R.; Schultz, M. J.; Mueller, J. A.; Sigman, M. S. *Angew. Chem., Int. Ed.* **2003**, *42*, 3810.
(10) Seiders, T. J.; Ward, D. W.; Grubbs, R. H. *Org. Lett.* **2001**, *3*, 3225.
(11) Alexakis, A.; Winn, C. L.; Guillen, F.; Pytkowicz, J.; Roland, S.; Mangeney, P. *Adv. Synth. Catal.* **2003**, *345*, 345.
(12) Roland, S.; Audouin, M.; Mangeney, P. *Organometallics* **2004**, *23*, 3075.
(13) Enders, D.; Geilen, H.; Breuer, K. *Tetrahedron: Asymmetry* **1997**, *8*, 3571.
(14) Powell, M. T.; Hou, D.-R.; Perry, M. C.; Cui, X.; Burges, K. *J. Am. Chem. Soc.* **2001**, *123*, 8878.
(15) Nielsen, R. J.; Keith, J. M.; Stoltz, B. M.; Goddard, W. A., III. *J. Am. Chem. Soc.* **2004**, *126*, 7967.

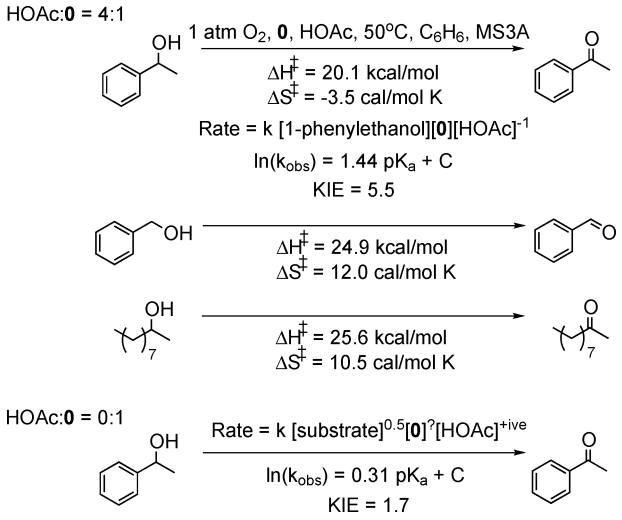

Figure 2. Summary of reactivity of (NHC)Pd(OAc)$_2$(H$_2$O), **0**, from ref 8.

NHCs for selectivity, we must know the geometry of the catalyst−substrate complex at the intended moment of enantioselection. In the simplest kinetic scheme, this will be the rate-limiting step (as in the case of (−)-sparteine catalysts), and an atomic-scale description of this step was the goal of this work.

Another factor which makes carbenes an attractive scaffold is the quantitative description of the reactivity of **0**, (1,3-bis-(2,6-diisopropylphenyl)imidazol-2-ylidene)Pd(OAc)$_2$(H$_2$O), available in ref 8 and summarized here (Figure 2). We expected that correlations between experimental and calculated data would yield a detailed understanding of substrate oxidation, minimizing the need for unsupported assumptions. Mueller et al. reported two regimes of reactivity in the aerobic oxidation of 1-phenylethanol by **0** and acetic acid in benzene at 50 °C: a high acetic acid concentration regime (acid:**0** ratio greater than ∼3:1) and a low acid concentration regime when no acid was added other than that generated in situ by reaction of substrate and **0**. As in previous systems, we expect that the acetate in this system deprotonates palladium-bound alcohols. Excess acetic acid, which necessarily drives this deprotonation equilibrium in reverse, was also found to stabilize the catalyst against decomposition at low (ambient) O_2 pressures. It was inferred by Mueller that the acid reduces the amount of (**A**)Pd^0 present by simultaneously driving the reaction forward (via protonation of (**A**)Pd(O_2) species) and backward (via oxidative addition of acetic acid), away from (**A**)Pd^0. Activation parameters in the high acid regime were measured for 1-phenylethanol and benzyl alcohol via Eyring plots between 40 and 55 °C. Despite their similar rates in this temperature range, there is a curious discrepancy between the contributions of entropy and enthalpy to the total activation free energy for the two substrates ($\Delta S^{\ddagger}_{1-\text{phenyl}} = -3.5$ eu, $\Delta S^{\ddagger}_{\text{benzyl}} = 12$ eu). We note that roughly the same difference in activation entropies was observed between these two substrates using the ((−)-sparteine)PdCl$_2$ catalyst.[16] Reaction rates varied inversely with acid concentration, were first-order in catalyst and 1-phenylethanol concentration, and were independent of O_2 pressure. In the absence of exogenous acetic acid, a half-order dependence on substrate concentration was observed. The authors also explored the effect of replacing the acetate groups in **0** (along with the excess acetic acid) with carboxylates of varying pK_a. At an acid:**0** ratio of 4:1, the rate of oxidation of 1-phenylethanol increases sharply with the carboxylic acid pK_a: $\log(k_{obs}) = 1.44\ pK_a + C$. In the absence of exogenous acid, this relationship became $\log(k_{obs}) = 0.31\ pK_a + C$.

A notable property of the reaction of **0** with 1-phenylethanol[17] is the unusually high kinetic isotope effect measured when the substrate is deuterated at the secondary carbon. Analogous KIEs measured using ((−)-sparteine)PdCl$_2$ (1.31[16]), (bathophenanthroline disulfonate)Pd(OAc)$_2$ (1.4[18]), and (pyridine)$_2$Pd(OAc)$_2$ (1.5[19]) were 1.5 or lower. **0** exhibited a KIE of 1.7 when no excess acetic acid was present in solution, but as the acid concentration was increased, the measured KIE rose to 5.5 at a Pd:acid ratio of 1:4 without reaching an asymptote. A value of 6.8 was reported earlier for the same catalyst.[9] This observation and the reaction orders suggested that, under conditions favorable for both rates and catalyst stability (Pd:HOAc ≈ 1:4), C−H$_\beta$ bond scission is rate-limiting in reactions with **0**, as it is for most other catalysts.[20] However, the KIE, along with the monodentate nature of the carbene ligand and its strong trans influence, urged us to consider new mechanistic possibilities beyond those relevant for ((−)-sparteine)PdCl$_2$.

After describing the calculation of thermodynamics in the next section, we introduce possible mechanisms of substrate oxidation. Comparisons are then drawn between computational results and the experimental kinetics data in order to elucidate the active mechanism. Implications of the theoretical results for possible enantioselective reactions are discussed before the Conclusions section.

2. Methods

Solution-phase enthalpies were calculated as

$$H = E_{\text{elec}} + G_{\text{solv}} + \sum_{\nu}\frac{1}{2}h\nu + \sum_{\nu}\frac{h\nu}{e^{h\nu/kT}-1} + \frac{n}{2}kT \qquad (1)$$

including the electronic energy, Poisson−Boltzmann solvation energy, zero-point energy, internal vibrational energy, and $^1/_2\,kT$ for each translational and rotational mode. Electronic energies and optimized structures are calculated with the B3LYP[22,23] collection of gradient-corrected density functionals and the 6-31G**[24,25] basis set, augmented with diffuse functions[26] on the two active hydrogen atoms, β-carbon, and all oxygen atoms. To calculate vibrational spectra and to locate transition states, we calculated analytic Hessians using the smaller 6-31G basis set, again augmented with polarization and diffuse functions on the listed atoms. Hessian calculations were performed on structures separately optimized using the reduced basis. Palladium was described using the Los Alamos[27] effective core potential with the double-ζ

(16) Mueller, J. A.; Sigman, M. S. *J. Am. Chem. Soc.* **2003**, *125*, 7005.

(17) Also observed with 2-decanol.
(18) ten Brink, G.-J.; Arends, I. W. C. E.; Sheldon, R. A. *Adv. Synth. Catal.* **2002**, *344*, 355.
(19) Measured using β-deuterated benzyl alcohol: Steinhoff, B. A.; Guzei, I. A.; Stahl, S. S. *J. Am. Chem. Soc.* **2004**, *126*, 11268.
(20) Exceptions may include the aerobic oxidation of benzylic alcohols by Pd(OAc)$_2$ in DMSO (reoxidation of reduced palladium initially proposed as rate-limiting: (a) Steinhoff, B. A.; Fix, S. R.; Stahl, S. S. *J. Am. Chem. Soc.***2002**, *124*, 766. (b) Zierkiewicz, W.; Privalov, T. *Organomet.* **2005**, *24*, 6019) and oxidations by triethylamine[21] and (−)-sparteine[16] complexes of palladium under base-deficient conditions (substrate deprotonation proposed as rate-limiting).
(21) Schultz, M. J.; Adler, R. S.; Zierkiewicz, W.; Privalov, T.; Sigman, M. S. *J. Am. Chem. Soc.* **2005**, *127*, 8499.
(22) Becke, A. D. *J. Chem. Phys.* **1993**, *98*, 5648.
(23) Lee, C.; Yang, W.; Parr, R. G. *Phys. Rev. B* **1988**, *37*, 785.
(24) Hehre, W. J.; Ditchfield, R.; Pople, J. A. *J. Chem. Phys.* **1972**, *56*, 2257.
(25) Hariharan, P. C.; Pople, J. A. *Theor. Chim. Acta* **1973**, *28*, 213.
(26) Frisch, M. J.; Pople, J. A.; Binkley, J. S. *J. Chem. Phys.* **1984**, *80*, 3265.
(27) Hay, P. J.; Wadt, W. R. *J. Chem. Phys.* **1985**, *82*, 299.

contraction of their basis set. Solvation energies were computed for the gas-phase optimized geometries using the Poisson−Boltzmann polarizable continuum method to represent benzene with $\epsilon = 2.22$ and effective radius 2.6 Å. For less critical intermediates, only a solvated energy is reported, $E_{sol} = E_{elec} + G_{solv}$.

When acetic acid leaves the sphere of palladium, it is assumed (for the purposes of calculating relative enthalpies) to exist in solution as hydrogen-bonded dimers. The equilibrium constant for dimerization in benzene ($K_{eq} \approx 400$ M^{-1} at 25 °C[28]) shows that dimers dominate the population at most acetic acid concentrations, but at the low loadings (0−0.01 M) explored by Mueller et al.,[8] free monomers become competitive. Even in this case, free water molecules[29] (either preexisting in the solvent, dissociated from **0**, or produced during reaction by the disproportionation of H_2O_2) can stabilize the acid as hydrated monomers.[28] Unreacted substrate molecules (initially present at 0.45 M) can also play this role. The calculated enthalpy of dimerization ($2HOAc \rightarrow (HOAc)_2$) is $\Delta H = -9.4$ kcal/mol. The calculated enthalpy change for the association of acetic acid and water ($H_2O + HOAc \rightarrow H_2O{\cdot}HOAc$, $\Delta H = -5.0$ kcal/mol) or 1-phenylethanol ($C_8H_9OH + HOAc \rightarrow C_8H_9OH{\cdot}HOAc$, $\Delta H = -3.9$ kcal/mol) suggests the same stabilization (within a kilocalorie per mole of acid). If the uncomplexed monomer is, indeed, the dominant state of acetic acid in situ, then the reported enthalpies of intermediates which have lost HOAc units should be uniformly raised by $^1/_2$ (9.4) = 4.7 kcal/mol. The C−H$_\beta$ bond scission activation enthalpies calculated this way (~22 kcal/mol for 1-phenylethanol) are not in contradiction with experiment, and our conclusions are not affected.

3. Results

Possible C−H$_\beta$ Bond Scission Transition States. Six geometries for C−H$_\beta$ bond scission were hypothesized and modeled using 1-phenylethanol as substrate. TS1 and TS2 (Figure 3) feature traditional β-hydride elimination from a Pd-bound alkoxide, leaving the hydride either cis (TS1) or trans (TS2) to the carbene ligand. Since the strong electron donation of carbene ligands discourages the formation of covalent bonds in the trans position, we also considered the possibility that the β-hydrogen passes directly from the substrate to the free oxygen of a coordinated acetate ligand (TS3). The products of this "reductive" β-hydride elimination are a molecule of acetic acid and a ketone-coordinated Pd(0) complex. In such a mechanism, no intermediates include covalent bonds trans to the carbene. Mueller et al. also proposed the direct transfer of hydrogen to oxygen as a possible explanation of the large kinetic isotope effect measured.[8] Failing to locate a representative transition-state structure with DFT, they dismissed this possibility based on the expected nucleophilicity of both the carboxylate ketone and hydride moieties. In contrast, we find a transition state with the geometry of TS3, including a direct interaction of the migrating hydrogen with the metal. This allows the mechanism to retain the pericyclic, symmetry-allowed nature of a β-hydride elimination, although the proton continues to the more thermodynamically stable location on the carboxylate.

Recent reports of C−H activation by late metal carboxylates or sulfates in which coordinated bases act as proton acceptors involve Pd^{II},[30] Ir^{III},[31] Pt^{II},[32] and Au^{III}.[33] Like the reductive

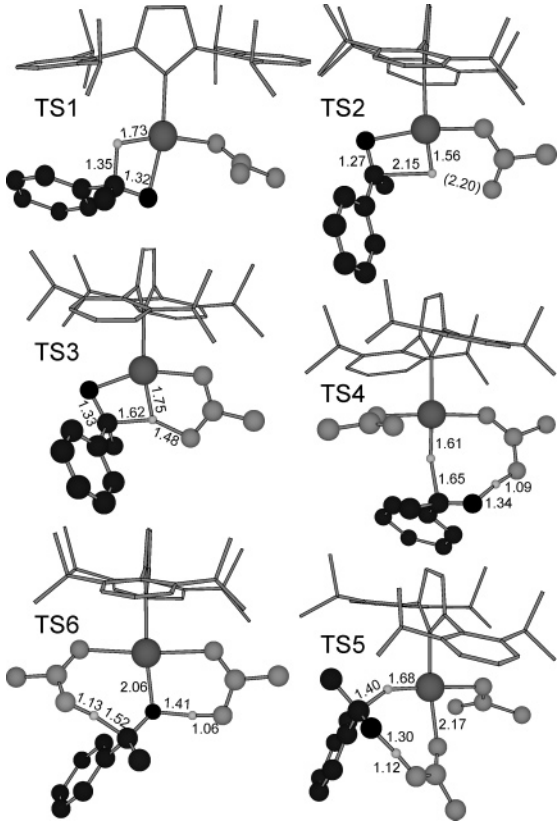

Figure 3. C−H$_\beta$ bond scission transition states modeled. Bond lengths in Å, inert hydrogen atoms are omitted, acetate groups shaded light, 1-phenylethanol shaded dark.

β-hydride elimination, these reactions feature vacancies provided by the dissociation of κ^2-oxygenates and bond cleavage promoted by intramolecular nucleophiles. The alkoxide we discuss here permits the formal reduction of the metal center, while in the electrophilic substitution reactions cited, the substrate provides a more electron-rich ligand than the departing carboxylate.

In TS4, TS5, and TS6, the substrate is dehydrogenated in one concerted step. TS4 and TS5 are analogous to the mechanism of Noyori dehydrogenatation,[34] in which the proton-like hydrogen is transferred to a coordinated base (acetate in this case) while the hydride-like hydrogen moves to the metal. To avoid the formation of a palladium hydride, the less traditional TS6 was also considered. Here, both hydrogen atoms are transferred to coordinated acetate groups, again producing acetic acid and Pd^0. (Transition states not involving C−H$_\beta$ activation will be denoted with a ‡.)

Thermodynamics and Kinetics. In examining the thermodynamics of the mechanisms implied by these transition states, the complex (**A**)Pd(OAc)$_2$ (**1**) was chosen as reference, along with free alcohol in solution and O_2 at 1 atm. Sigman et al.[8] showed by NMR that, in benzene, the bound water of **0** is dissociated above 0 °C. Relaxation of **1** shows that the resulting vacancy is filled by a dative bond from a κ^2-acetate anion. Incorporating an explicit solvent molecule showed that the steric crowding around the metal renders a π-adduct (**A**)Pd(OAc)$_2$-(C_6H_6) *less* stable than **1** by 7.5 kcal/mol in enthalpy.

(28) Fujii, Y.; Yamada, H.; Mizuta, M. *J. Phys. Chem.* **1988**, *92*, 6768.
(29) The solubility of water in benzene at 25 °C is 0.035 M ((a) Christian, S. D.; Affsprung, H. E.; Johnson, J. R. *J. Chem. Soc.* **1963**, 1896. (b) Masterton, W. L.; Gendrano, M. C. *J. Phys. Chem.* **1966**, *70*, 2895), though the molecular sieves present will sequester free water.
(30) Davies, D. L.; Donald, S. M. A.; Macgregor, S. A. *J. Am. Chem. Soc.* **2005**, *127*, 13754.
(31) Davies, D. L.; Donald, S. M. A.; Al-Duaij, O.; Macgregor, S. A.; Pölleth, M. *J. Am. Chem. Soc.* **2006**, *128*, 4210.
(32) Ziatdinov, V. R.; Oxgaard, J.; Mironov, O. A.; Young, K. J. H.; Goddard, W. A., III; Periana, R. A. *J. Am. Chem. Soc.* **2006**, *128*, 7404.
(33) Jones, C. J.; Taube, D.; Ziatdinov, V. R.; Periana, R. A.; Nielsen, R. J.; Oxgaard, J.; Goddard, W. A., III. *Angew. Chem., Int. Ed.* **2004**, *43*, 4626.
(34) Hashiguchi, S.; Fujii, A.; Takehara, J.; Ikariya, T.; Noyori, R. *J. Am. Chem. Soc.* **1995**, *117*, 7562.

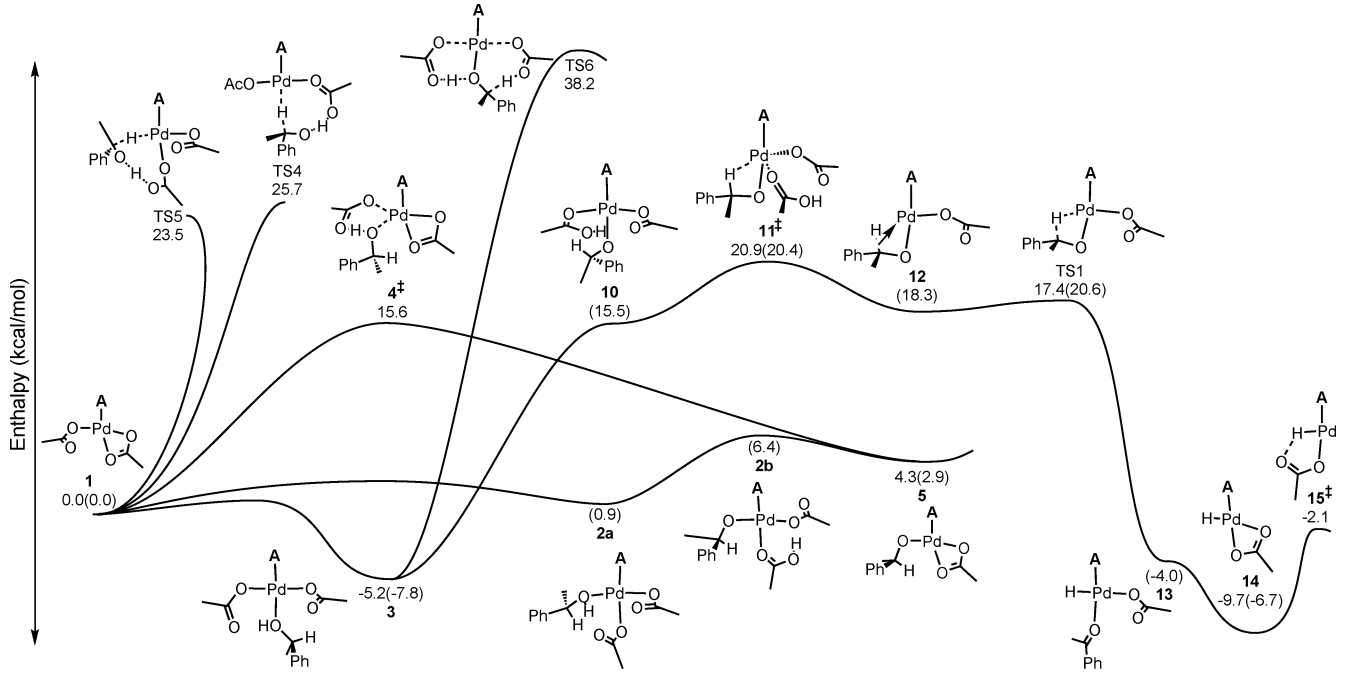

Figure 4. Possible mechanisms for the oxidation of 1-phenylethanol by (**A**)Pd(OAc)$_2$. Enthalpies (kcal/mol) at 60 °C include solvation by benzene (ϵ = 2.22). Energies (E_{sol}) are given in parentheses since enthalpies were not calculated for all intermediates. Images are projections of the 3D structures.

Passage through TS4 or TS5 does not require prior coordination of the substrate to the catalyst, only the creation of a vacancy. These dehydrogenation paths lie 25.7 (TS4) and 23.5 kcal/mol (TS5) above state **1** (Figure 4). 1-Phenylethanol can coordinate to the metal via multiple paths. The substrate may displace the dative bond from acetate and coordinate trans to the carbene, as in **3**. Despite the exothermicity of this substitution, the entropic penalty of immobilizing free substrate is expected to make state **1** dominate the **1** ⇌ **3** equilibrium. If this were not the case, we would expect a zeroth-order dependence of rate on substrate instead of the observed first-order dependence. TS6 is accessible from **3**, though its calculated enthalpy ($\Delta H^{\ddagger}$ = 38.2 kcal/mol) shows that it is not a viable reaction pathway.

The substrate can also coordinate cis to the carbene by displacing the κ^1-coordinated acetate ion. The associative substitution of alcohol for acetate is simultaneous with the deprotonation of the alcohol. The imaginary normal mode of **4**‡ (with frequency 100*i* cm^{-1}) is composed of the translation of the alcohol and acetate relative to the metal fragment. An intrinsic reaction coordinate (minimum energy pathway) calculation from **4**‡ confirms that the deprotonation continues exothermically, yielding the Pd−alkoxide **5** after loss of the acetic acid molecule. The barrier to this displacement ($\Delta H^{\ddagger}$ = 15.6 kcal/mol) is considerable but not as large as the barriers posed by C−H$_\beta$ bond-breaking reactions.

A lower-enthalpy path for coordinating the substrate cis to the carbene may avoid the simultaneous substitution−deprotonation step. Sequential coordination of substrate (**2a**), intramolecular deprotonation to form **2b**, and dissociation of acetic acid also leads to the alkoxide **5**. Similar sequential alternatives may also be relevant to discussions of related catalysts.[21]

The β-hydride elimination transition state TS1 also has a low enthalpy of $\Delta H^{\ddagger}$ = 17.4 kcal/mol. However, we find that, no matter how the reactants approach this configuration, it will not provide the highest barrier of the mechanism. TS1 separates the coordinately unsaturated Pd−alkoxide **12** from the Pd−hydride **13**. This reaction step is so exothermic and the transition state so early that TS1 poses essentially no barrier relative to **12**. (If the Pd−hydride **13** is stabilized by replacing acetate with a more electron-withdrawing carboxylate, such as *m*-chlorobenzoate or trifluoroacetate, **12** becomes altogether unstable and relaxes directly to **13**.) Further reaction of the Pd−hydride **13** via dissociation of the ketone (**14**) and reductive elimination[35] of acetic acid (**15**‡) follows. This indicates that the rate-limiting step of a mechanism featuring TS1 lies before **12**.

The alkoxide **12** can be generated by the elimination of acetic acid from state **3**. Transfer of a proton from the bound alcohol to an acetate ligand in **3** yields the Pd−alkoxide **10**. Through the associative substitution **11**‡, the bound acetic acid unit is replaced by a β-agostic interaction with the C−H$_\beta$ bond (**12**). **11**‡ is expected to provide the rate-limiting barrier of this pathway, with an activation enthalpy of 20.9 kcal/mol. A low-energy rearrangement of the Pd−alkoxide **5** to form **12** has not been identified.

The Pd−alkoxide **5** precedes both TS2 and TS3 (Figure 5). In the β-hydride elimination step TS2, the oxygen trans to the carbene is not involved in the reaction after being displaced from the metal. It is also evident from the geometry of TS2 (Figure 3) that this is a very late transition state, consistent with the endothermicity of forming a Pd−hydride trans to the carbene ligand in **6**. Intermediate **6** becomes stable only after the Pd−O−C$_\beta$−C$_{phenyl}$ torsion angle twists such that the π-orbitals of the O=C$_\beta$ bond cease to overlap the Pd−H bond. Given the small barrier ($\Delta H^{\ddagger}$ = 3.2 kcal/mol) for the reverse reaction of **6** to TS2, it is unlikely that the reaction can proceed forward from **6** through a transition state with a lower enthalpy than

(35) We will use "reductive elimination" to describe the departure of acetic acid from a Pd−hydride intermediate, although we feel this process is electronically closer to acid−base reactivity (a proton hopping from one pair of electrons on palladium to another on the free carboxylate oxygen) than to traditional reductive elimination (a single orbital changing in character from antibonding between two adjacent ligands to a metal lone-pair as the ligands form a bond).

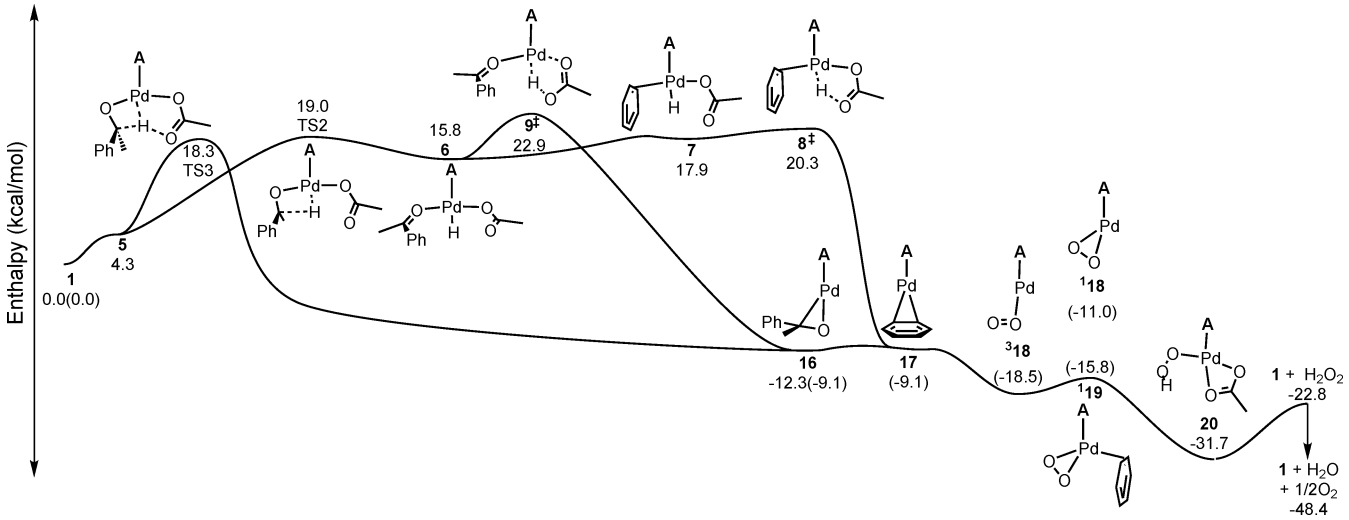

Figure 5. Possible mechanisms for the oxidation of 1-phenylethanol by (**A**)Pd(OAc)$_2$. Enthalpies (kcal/mol) at 60 °C include solvation by benzene (ϵ = 2.22). Energies (E_{sol}) are given in parentheses. Images are projections of the 3D structures.

TS2. Reductive elimination of acetic acid through **9**‡ poses an overall barrier of $\Delta H^{\ddagger} = 22.9$ kcal/mol. While greater than the barrier associated with TS2, this value is not far from the observed activation enthalpy of 20.1 kcal/mol. Alternatively, the ketone in **6** can be displaced by solvent (**7**) before reductive elimination of acetic acid in **8**‡ ($\Delta H^{\ddagger} = 20.3$ kcal/mol). Without accurate free energies, it is not possible to determine which transition state (TS2, **8**‡, **9**‡) would characterize the kinetics of a reaction through TS2 on the basis of thermodynamic calculations alone. Since the stereocenter of the substrate is destroyed before the reductive elimination steps, a chiral ligand could not be designed to exert enantioselectivity on these steps. The possibility of rate limitation by **8**‡ or **9**‡ is therefore a critical issue.

TS3 combines the β-hydride elimination from the alkoxide with the reductive elimination of acetic acid from palladium in one step, with the lowest barrier yet calculated ($\Delta H^{\ddagger} = 18.3$ kcal/mol). The short Pd−H distance (1.75 Å) in TS3 suggests that the $d_{x^2-y^2}$ orbital lobe trans to the carbene, while unfavorable for hosting the hydride as an intermediate, does stabilize the transit of the hydrogen from carbon to oxygen and accept the two electrons from the C−H$_\beta$ bond. TS3 leads to the (**A**)Pd^0-(ketone) complex **16**.

Pd^0, produced by substrate oxidation, is expected to exist mainly as the benzene adduct **17**, no less stable than **16**. The interaction of dioxygen and reduced palladium species has been examined recently.[36−38] Here, it is apparent that adsorption of triplet dioxygen on the (**A**)Pd^0 fragment (^{3}**18**) is aided by charge transfer into the antibonding orbitals of O_2 (0.36 e$^-$ by Mulliken populations, O−O bond length of 1.29 Å). The η^1 coordination geometry of this Pd^0 complex is reminiscent of a stable Cu^I−O_2 complex studied spectroscopically and theoretically.[39] The singlet intermediate ^{1}**18**, available through a spin-transition, assumes a pseudo-square-planar geometry which is stabilized by a dative bond from a solvent molecule, as in ^{1}**19**. (The linear

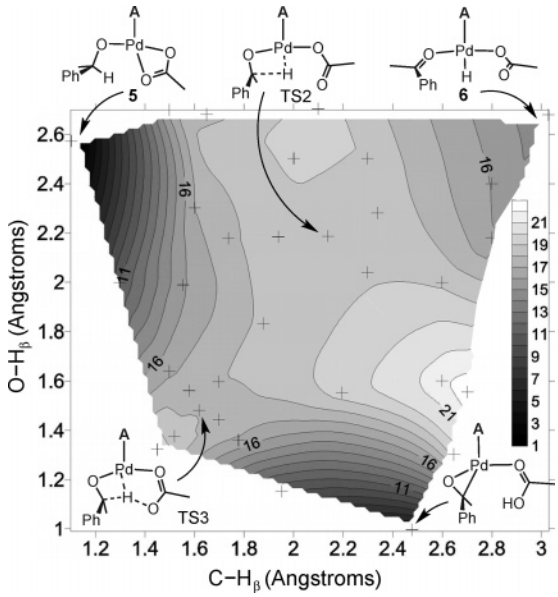

Figure 6. Potential energy surface spanned by C−H$_\beta$ and H$_\beta$−O$_{Ac}$ bond distances. Energies (kcal/mol) are gas-phase values calculated with the augmented 6-31G basis set (see Methods), relative to the Pd−alkoxide **5**. Plusses mark data points used for interpolation.

^{3}**18** does not bond to an explicit solvent molecule.) Generation of the hydroperoxide intermediate **20** is exothermic en route to the regenerated diacetate complex **1**. The calculated net reaction enthalpy, assuming a hydrogen peroxide product, is $\Delta H = -22.8$ kcal/mol, but this becomes −48.4 kcal/mol after disproportionation of the peroxide to water and dioxygen. The comparable free energies of **17**, ^{3}**18**, and the most stable palladium hydride complex, **14** (bearing in mind the greater entropic penalty of immobilizing O_2), corroborate Mueller's assertion[8] that free acetic acid stabilizes the catalyst against precipitation of palladium black by driving the **14** ⇌ ^{3}**18** equilibrium away from Pd^0.

The reactions **5** → TS2 → **6** and **5** → TS3 → **16** can be represented on the same two-dimensional potential energy surface (PES) spanned by the C−H$_\beta$ and H$_\beta$−O$_{Ac}$ bond lengths. The PES in Figure 6 is constructed from gas-phase energies calculated with the augmented 6-31G basis set by constraining these two internal coordinates to different values and allowing all other coordinates to relax. During the reaction through TS2,

(36) Landis, C. R.; Morales, C. M.; Stahl, S. S. *J. Am. Chem. Soc.* **2004**, *126*, 16302.
(37) Konnick, M. M.; Guzei, I. A.; Stahl, S. S. *J. Am. Chem. Soc.* **2004**, *126*, 10212.
(38) Keith, J. M.; Nielsen, R. J.; Oxgaard, J.; Goddard, W. A., III. *J. Am. Chem. Soc.* **2005**, *127*, 13172.
(39) Schatz, M.; Raab, V.; Foxon, S. P.; Brehm, G.; Schneider, S.; Reiher, M.; Holthausen, M. C.; Sundermeyer, J.; Schindler, S. *Angew. Chem., Int. Ed.* **2004**, *43*, 4360.

Table 1. Comparison of Carbene **A** and Pyridine

	enthalpy (kcal/mol)							
ligand	**1**[a]	**3**	TS1	**5**	TS3	TS2	**6**	**9**‡
A	0.0	−5.2	17.4	4.3	18.3	19.0	15.8	22.9
pyridine	0.0	−10.1	14.5	−0.5	−[b]	10.7	1.2	8.9

[a] For structures, see Figures 4 and 5. [b] No saddle point corresponding to TS3 exists on the potential surface when L = pyridine.

the $H_\beta-O_{Ac}$ distance remains large as $C-H_\beta$ increases from 1.10 Å in **5** to 3.19 Å in **6**. Note that the gradient of the surface around TS2 is very gentle in both dimensions. The $H_\beta-O_{Ac}$ distance is not constrained by any bonding interaction, leaving this reaction channel broad perpendicular to the reaction coordinate. The energy profile with respect to the $C-H_\beta$ coordinate is governed by the formation of the weak Pd−H bond in **6**, so the barrier which must be crossed is very wide parallel to the reaction coordinate as well. The imaginary vibrational frequency calculated at TS2 is only $14i$ cm^{-1}. When Mueller et al.[8] located TS2, they found a $C-H_\beta$ distance of 1.97 Å, which according to Figure 6 implies essentially no difference in activation energy. On the other hand, the curvature around TS3, both parallel and perpendicular to the reaction coordinate, is pronounced. The energy profile is determined by the formation and breaking of strong C−H and O−H bonds, and the imaginary vibrational frequency at TS3 is $999i$ cm^{-1}.

Mulliken charges on the migrating hydrogen in states **5** (+0.07), TS3 (+0.25), TS2 (+0.10), **6** (+0.04), and **9**‡ (+0.23) remain positive, and atomic charges fit to the species' electrostatic potentials fall within a quarter electron of these. These charges suggest that the negative charge implied by the hydride label is physically misleading in the context of the late metals whose electronegativities match that of hydrogen. The utility of considering the metal-bound hydrogen as acidic is also supported by the reactivity trend calculated below, that more basic carboxylates yield lower barriers in the reductive elimination of carboxylic acids from Pd−hydrides (e.g., **6** → **9**‡).

The reductive β-hydride elimination mechanism has not been considered in discussions of related palladium catalysts featuring imines, amines, BINAP, or DMSO (i.e., non-carbenes) as ligands. Its appearance as a tenable mechanism in the case of carbene-ligated catalysts can be traced to the effect of carbenes' strong σ-donation on the potential energy surface. This effect is illustrated in Table 1 by comparing the calculated enthalpies of intermediates and transition states incorporating either carbene **A** or pyridine as the neutral ligand and 1-phenylethanol as substrate. The traditional β-hydride elimination transition state, which leaves the hydride trans to acetate (TS1), is only slightly lower in enthalpy relative to **1** in the case of pyridine. The energy profiles are much more distinct near the formation or elimination of a hydride trans to the neutral ligand. The palladium hydride **6** is 14.6 kcal/mol lower in enthalpy (relative to **1**) for pyridine than for **A**. Differences of this magnitude are more than enough to cause qualitative changes in reaction mechanisms. Due to the stability of the hydride trans to pyridine, the β-hydride elimination transition state TS2 becomes the lowest-enthalpy $C-H_\beta$ activation route (even lower than the isomeric TS1). The following elimination of acetic acid (**9**‡) poses a lower barrier than $C-H_\beta$ activation in the pyridine system. In terms of the PES in Figure 6, the reaction manifold **5** → TS2 → **6** → **9**‡ is so stabilized that TS3 no longer exists as a separate saddle point but is "absorbed" by TS2. In the case of pyridine, TS2 features a shorter $C-H_\beta$ bond length of 1.61 Å. (Note that these intermediates are not intended as a complete description of the $Pd(OAc)_2$/pyridine catalytic cycle, which features a resting state including two pyridine molecules.[19])

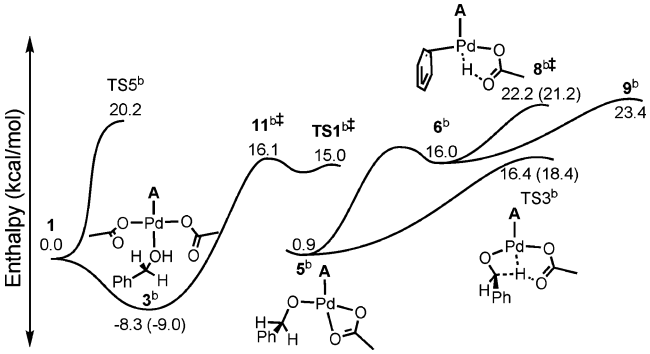

Figure 7. Possible intermediates in the oxidation of benzyl alcohol by (**A**)$Pd(OAc)_2$. Enthalpies (kcal/mol) at 60 °C include solvation by benzene ($\epsilon = 2.22$). Enthalpies of analogous complexes incorporating 2-decanol as substrate are in parentheses.

Thermodynamic properties of key intermediates in the oxidation of benzyl alcohol by **1** are shown in Figure 7. The calculated enthalpies of most intermediates incorporating benzyl alcohol are ∼3 kcal/mol more stable relative to **1** and free substrate than for 1-phenylethanol. However, when measured experimentally, benzyl alcohol yielded a *higher* $\Delta H^‡$ and higher $\Delta S^‡$ than 1-phenylethanol (Figure 2). Together, the data suggest that the resting state of the catalytic cycle shifts from **1** when 1-phenylethanol is substrate to **3**[b] for benzyl alcohol. **1** is calculated to bind benzyl alcohol 3.1 kcal/mol more strongly than 1-phenylethanol (**3**[b] vs **3**). Although the $C-H_\beta$ activation barriers calculated for benzyl alcohol are lower than those for 1-phenylethanol relative to **1**, the predicted activation enthalpy in this scenario would be $\Delta H^‡(\mathbf{3}^b \rightarrow TS3^b) = 24.7$ kcal/mol, in agreement with the experimental value of 24.9 kcal/mol. A shift in resting state also explains the disparate activation entropies: $\Delta S^‡$(benzyl) is greater than $\Delta S^‡$(1-phenyl) because the unimolecular resting state **3**[b] has a lower entropy than the bimolecular resting state **1** + 1-phenylethanol. This explanation can be easily tested experimentally. A transition from zeroth-order to first-order dependence on [benzyl alcohol] is expected as the substrate concentration is lowered enough to drive the **1** ⇌ **3**[b] equilibrium back to **1**. Such a transition has been reported for $(pyridine)_2Pd(OAc)_2$[19] and $(triethylamine)_2Pd(OAc)_2$[21] catalysts and attributed to a pre-equilibrium between free substrate and a catalyst−substrate complex. The measured activation entropy of 2-decanol is also consistent with this shift in resting state. The activation enthalpy calculated for this reaction, $\Delta H^‡(\mathbf{3}^{dec} \rightarrow TS3^{dec}) = 27.4$ kcal/mol, agrees with the measured value of 25.6 kcal/mol. Since the ((−)-sparteine)$PdCl_2$ complex was also calculated to bind benzyl alcohol (as a palladium alkoxide) 3 kcal/mol more strongly than 1-phenylethanol, the same shift in resting state could explain the activation parameters measured using that catalyst (for 1-phenylethanol, $\Delta H^‡ = 16.8$ kcal/mol, $\Delta S^‡ = -17.1$ cal/(mol K); for benzyl alcohol, $\Delta H^‡ = 20.3$ kcal/mol, $\Delta S^‡ = -5$ cal/(mol K)).[16] For both benzyl alcohol and 2-decanol, the enthalpy of TS3 is lower than that of the alternative elimination of acetic acid, **8**‡.

While reaction (of 1-phenylethanol) through TS6 can be ruled out solely on the basis of thermodynamics, TS4, TS5, and **11**‡

Table 2. Enthalpies Calculated with Expanded Basis Set[a]

state	**1**	TS3	TS2	**6**	**8**‡	**9**‡
enthalpy (kcal/mol)	0.0	17.6	18.4	15.4	21.7	24.7

[a] Basis set described in text. Temperature-dependent terms from Hessian calculated with augmented 6-31G basis set.

cannot be discounted on their calculated enthalpies alone, given the accuracy of DFT. However, besides their higher enthalpies, these transition states will have lower entropy than TS2, **8**‡/**9**‡, and TS3, from which a molecule of acetic acid has already been liberated. To within the accuracy of the calculations, the activation enthalpies of **11**‡, TS2, **8**‡, and TS3 match each other and the measured $\Delta H^{\ddagger}$ of 20.1 kcal/mol, with that of **9**‡ lying slightly higher. We hypothesized that the finite nature of basis sets used in our calculations would artificially penalize the energy of TS3 (due to its greater number of long, half-formed bonds) more than other species. Accordingly, the key intermediates and transition states were reoptimized using a larger basis: cc-PVTZ++[40] on oxygen, active hydrogen, and β-carbon atoms; the triple-ζ contraction of the Los Alamos[27] basis and pseudopotential on palladium; 6-31G** on the remaining atoms. Following geometry optimization, electronic and solvation energies were evaluated with this enlarged basis plus a shell of f-orbitals[41] on palladium. At this level, structure TS3 is 7.1 kcal/mol lower in enthalpy than **9**‡ and 4.1 kcal/mol below **8**‡ (Table 2). From the gas-phase Hessians, the vibrational entropy of TS3 is calculated to be 5.9 eu lower than that of **9**‡. This is consistent with the extra rotational freedom of the bound ketone in **9**‡ (although our gas-phase Hessian cannot include the entropic effects for librational motions within the solvent shell of the condensed system). Our best estimate then is that TS3 is 7.1 kcal/mol − 323 K(5.9 eu) = 5.1 kcal/mol lower in free energy than **9**‡. Since state **8**‡ has the ketone replaced with solvent, the relative free energy of this state will depend on the activity of product and solvent. Considering only internal vibrational degrees of freedom, states **8**‡ and **9**‡ are calculated to have the same entropy. Considering the concentration of species under real reaction conditions, the free energy of **8**‡ will therefore be comparable to or below those of TS2 and TS3. In the following sections, other means of validating one mechanism are sought.

For relating calculated thermodynamics with the observed dependence of rates on isotopic substitution and carboxylate pK_a, rate laws are necessary. The simple network below can be used to derive rate laws for the various possible mechanisms,

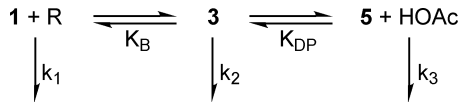

which must reproduce the reaction orders measured at a high HOAc:Pd ratio (first-order in substrate [R] and total catalyst $[Pd]^0$, inverse first-order in exogenous acid $[HOAc]^0$). If the release and exergonic disproportionation of hydrogen peroxide reaches equilibrium, catalyst states preceding **1** can be ignored. k_1, k_2, and k_3 are the elementary rates for reaction through TS4 or TS5, **11**‡ or TS6, and TS2 or TS3, respectively.[42]

(40) Dunning, T. H., Jr. *J. Chem. Phys.* **1989**, *90*, 1007.
(41) Ehlers, A. W.; Böhme, M.; Dapprich, S.; Gobbi, A.; Höllwarth, A.; Jonas, V.; Köhler, K. F.; Stegmann, R.; Veldkamp, A.; Frenking, G. *Chem. Phys. Lett.* **1993**, *208*, 111.

Assuming added palladium and acetic acid are conserved according to $[Pd]^0 = [\mathbf{1}] + [\mathbf{3}] + [\mathbf{5}]$ and $[HOAc]^0 = [HOAc]$ at high acid:Pd ratios, rates limited by k_1, k_2, or k_3 can be derived:

$$\text{rate}_1 = k_1[R][Pd]^0 \tag{2}$$

$$\text{rate}_2 = k_2K_B[R][Pd]^0 \tag{3}$$

$$\text{rate}_3 = \frac{k_3K_BK_{DP}[R][Pd]^0}{[HOAc]^0} \tag{4}$$

In each case, state **1** must be assumed the dominant palladium species (i.e., $1 \gg K_B[R] + K_BK_{DP}[R]/[HOAc]$) to ensure a first-order dependence on [R]. Since no acid is liberated before transition states **11**‡ or TS4−6, these paths do not yield the observed inverse dependence on $[HOAc]^0$. In itself, this argues against the relevance of these routes, but eqs 2 and 3 will nonetheless be used below in arguments regarding KIEs and carboxylate pK_a dependence. In each case, the free energy difference on which rates depend is simply the free energy difference between the rate-limiting transition state and state **1**.

Kinetic Isotope Effect. For comparison with the KIE of 5.5 measured using β-deuterated 1-phenylethanol[8] (6.8 reported in ref 9), a kinetic isotope effect was predicted for each of the possible rate-limiting steps considered. In each case, the free substrate is considered the ground state to which the transition state's thermodynamic properties are compared. However, since the vibrational properties of the β-hydrogen are little different in the Pd−alcohol complex **3** and the Pd−alkoxide **5**, KIE predictions made taking either of these states as reference are within half a unit of those shown. "Semiclassical" KIEs were predicted using only the difference in free energies of reaction for the two isotopomers:

$$\text{KIE}_{S-C} = \frac{k_H}{k_D} = \frac{\frac{kT}{h}\exp\left(-\frac{\Delta G_H^{\ddagger}}{RT}\right)}{\frac{kT}{h}\exp\left(-\frac{\Delta G_D^{\ddagger}}{RT}\right)} \tag{5}$$

Here, $\Delta G^{\ddagger}$ includes the mass-dependent components' zero-point energy, internal vibrational energy, and internal vibrational entropy, all evaluated using the appropriately mass-weighted gas-phase Hessian. Since the transition states under consideration involve the motion of light atoms, we have also considered the likelihood of tunneling contributing to reaction rates and therefore KIEs. Skodje and Truhlar derived an analytical expression (eq 21 of ref 43) for approximating the thermally averaged transmission coefficient κ appropriate for a parabolic barrier. Such a coefficient relates the probabilities of a wave passing over, tunneling through, or being reflected by a barrier and can be used to estimate the extent to which a rate calculated by classical transition-state theory will be augmented by quantum mechanical tunneling. Since

$$k_{QM} = \frac{kT}{h}\exp\left(-\frac{\Delta G^{\ddagger}}{RT}\right)\kappa \tag{6}$$

one can write

$$\mathrm{KIE_{QM}} = \mathrm{KIE_{S-C}}\frac{\kappa_H}{\kappa_D} \quad (7)$$

The only parameters used in estimating κ are the temperature (50 °C), barrier height (measured from the preceding stable intermediate), and barrier curvature (width). The width of the parabolic barrier is assumed to be related inversely to the imaginary eigenvalue of the mass-weighted Hessian. Reducing a highly dimensional potential energy surface to a one-dimensional parabola along the reaction coordinate is a severe approximation, especially for those segments of the reaction coordinate which are not characterized by the transfer of hydrogen between heavier groups. We are interested not in the quantitative value of the calculated transmission coefficients, but in a qualitative interpretation of the ratio κ_H/κ_D. When this ratio is near unity, the semiclassical KIE will not be enhanced by tunneling. Because of the exponential decay of wave functions under barriers, transmission coefficients (and κ_H/κ_D) will increase suddenly as the height or width of a barrier begins to allow tunneling.[44]

Properties of the transition states examined (summarized in Table 3) show a variety of responses to isotopic substitution. In **11**‡ (the displacement of an acetic acid molecule from Pd by the C−H_β bond), motion along the reaction coordinate involves the entire substrate and acid molecule. Hence, $\nu^‡$ is isotope-independent, and tunneling is negligible. The KIE of 1.8 indicates initial activation of the C−H_β bond, which is elongated to 1.18 Å in **11**‡ from 1.10 Å in free 1-phenylethanol.

The β-hydride elimination TS2, on the other hand, involves complete C−H_β bond cleavage and is accompanied by a $\mathrm{KIE_{S-C}}$ of 3.2. (Mueller et al. calculated a value of 3.8 for the same pathway.) The Pd−H bond has essentially formed in TS2, and the normal-mode analysis shows a Pd−H stretch at 1966 cm^{-1} and two orthogonal C_{ligand}−Pd−H bends[45] around 600 and 800 cm^{-1}. The reductive β-hydride elimination TS3 displays an even higher $\mathrm{KIE_{S-C}}$ of 6.2 because TS3 loses less zero-point energy upon deuteration. In TS3, the hydrogen is only involved in a Pd−H stretch near 1600 cm^{-1} and a bend at 1014 cm^{-1} both orthogonal to translation along the reaction coordinate. Since paths TS2 and TS3 have similar activation energies, the tunneling contribution to each is determined by the barrier thickness. This property is qualitatively illustrated in Figure 6 and quantified by the widely disparate imaginary frequencies $\nu^‡$ in Table 3. Whether the tunneling contribution κ_H/κ_D is quantitative or not, the reductive β-hydride elimination pathway is capable of exhibiting the large KIE observed experimentally, and perhaps larger if reaction conditions are manipulated to isolate the intrinsic effect.

A catalytic cycle including TS2 is expected to proceed through the reductive elimination of acetic acid in **8**‡ or **9**‡. While TS2 is predicted to be incapable of manifesting the experimentally observed KIE, **9**‡ is. Since the kinetic properties of the higher (rate-limiting) barrier would be observed, this pathway is therefore also capable of yielding the high KIE measured. (The vibrational properties of transition states **8**‡ and **9**‡ depend on how late the transition state lies along the reaction coordinate. Analogues of both **8**‡ and **9**‡, in which acetate is replaced with trifluoroacetate, feature longer H···Pd distances and $\mathrm{KIE_{S-C}}$'s greater than 6.)

Table 3. Summary of Kinetic Isotope Effect (KIE) Predictions

transition state	$\nu_H^‡$ ($\nu_D^‡$) (i cm^{-1})	$\mathrm{KIE_{S-C}}$	κ_H/κ_D
11‡	37 (37)	1.8	1.00
TS2	14 (14)	3.2	1.00
8‡	98 (97)	3.4	1.00
9‡	666 (525)	6.0	1.17
TS3	999 (735)	6.2	1.72
TS4	447 (430)	3.7	1.01
TS5	763 (738)	3.0	1.04
TS6	1208 (947)	4.6	2.53
4‡	100 (99)	1.2	1.00

The KIEs predicted for the concerted mechanisms TS4 and TS5 are below the experimental value of 5.5. TS6 (in which both the active hydrogen atoms of the alcohol are transferred to acetate groups) features a linear C···H_β···O_{Ac} geometry which, like that of TS3, fosters a high $\mathrm{KIE_{S-C}}$ and high $\nu^‡$. The high ratio κ_H/κ_D for TS6 is due to its high barrier (the tunneling rate is large *relative* to the classical rate), but this pathway is irrelevant for the same reason.

These results raise the question of whether the modest KIEs (1.3−1.5) recorded in alcohol oxidations using other palladium catalysts represent C−H_β bond scission, formation of a β-agostic interaction, or a convolution of multiple steps.

Rate Dependence on pK_a. Mueller et al.[8] prepared a series of (**A**)Pd(carboxylate)$_2$(H_2O) complexes with carboxylates representing a range of basicity. The rate of 1-phenylethanol oxidation by these catalysts was measured under high acid concentrations, yielding the relation $\log(k_{obs}) = 1.44(\pm 0.13)\ \mathrm{p}K_a + C$. Substituting $A_o \exp(-\Delta G^‡/kT)$ for k_{obs} and rearranging yields

$$1.44\ \mathrm{p}K_a = \frac{-\Delta G^‡}{2.303kT} + C \quad (8)$$

or, at $T = 50$ °C,

$$\Delta G^‡ = -2.13(\pm 0.19)\ \mathrm{p}K_a + C \quad (9)$$

We calculated activation energies for possible rate-limiting transition states employing a number of carboxylates. We sought to corroborate or discredit the proposed pathways by comparing the dependence of their predicted activation energies on pK_a with eq 9. To avoid the assumptions associated with using frequencies calculated in the gas phase for solution-phase entropies, Table 4 reports activation enthalpies and energies. Since electronic effects are responsible for the changes in rate observed here, it is reasonable to expect $\Delta H^‡$ and $\Delta E_{sol}^‡$ to capture the pK_a-dependence of rates. The accuracy of solution-phase entropy calculations notwithstanding, we note that, for

(42) Due to their instability relative to preceding states, accumulation of **6** and **7** will be negligible.
(43) Skodje, R. T.; Truhlar, D. G. *J. Phys. Chem.* **1981**, *85*, 624.
(44) Recall that quantum mechanical penetration of a barrier tends to decrease exponentially with (width)[2(mass)(height)]$^{1/2}$; i.e., barrier width is weighted more heavily than height.
(45) It may seem contradictory that there are three hydrogen-dominated modes *in addition* to the imaginary eigenvector. The motion along the reaction coordinate at TS2 is actually dominated by the ketone, as the O═C bond twists away from the Pd−H bond and a long hydrogen bond forms between a hydrogen on the substrate phenyl group and the free oxygen of the acetate ligand. The flatness of the PES near TS2 and the large mass of the ketone are responsible for the small magnitude of $\nu^‡$.

Table 4. $\Delta H^{\ddagger}$ (and $\Delta E_{sol}^{\ddagger}$)[a] of Transition States as a Function of Carboxylate pK_a

carboxylate	acid pK_a	**11**‡	TS3	TS2	**8**‡	**9**‡	log(k_{obs})[b]
$(H_3C)_3C-COO^-$	5.03	22.2 (21.7)	16.9 (20.1)	19.2 (22.2)	18.8 (21.4)	20.6 (24.0)	-3.72
H_3C-COO^-	4.76	20.9 (20.4)	18.3 (21.4)	19.0 (21.2)	20.3 (22.7)	22.9 (27.0)	-4.18
$(C_6H_5)-COO^-$	4.19	20.5 (20.8)	17.5 (20.7)	17.4 (20.0)	− (−)	− (−)	−4.86
F_3C-COO^-	0.3	18.6 (19.1)	25.3 (29.3)	20.8 (23.9)	27.4 (31.2)	29.5 (35.1)	−[c]
d($\Delta H^{\ddagger}$)/d(pK_a) (d($\Delta E_{sol}^{\ddagger}$)/d(p$K_a$)):		0.6 (0.4)	−1.7 (−1.9)	2.3 (2.6)[d]	−1.7 (−2.0)	−1.7 (−2.1)	

[a] Values are ΔH (ΔE_{sol}), in kcal/mol, relative to the (**A**)Pd(carboxylate)$_2$ complex. [b] From ref 8; HOAc:Pd = 4:1. [c] Not reported. [d] TS2 does not show a linear dependence of $\Delta H^{\ddagger}$ on pK_a; fit neglects trifluoroacetate datum.

TS3, the calculated free energy dependence d($\Delta G^{\ddagger}$)/d(pK_a) = −1.79 matches the enthalpy dependence d($\Delta H^{\ddagger}$)/d(pK_a) = −1.74.[46]

Of **11**‡, TS2, and TS3, only TS3 is consistent with the strong dependence of rate on basicity. Since both carboxylates of the (**A**)Pd(carboxylate)$_2$ complex have accepted or are accepting protons in this state, it is intuitive that more basic carboxylates will lower the associated activation barrier. As noted by the experimentalists,[8] β-hydride elimination barriers are expected to *increase* with carboxylate basicity, since more-electron-rich anions decrease the electrophilicity of the palladium center. Neglecting the case of trifluoroacetate, the activation enthalpies of TS2 follow this trend.

Activation barriers for the reductive elimination of a carboxylic acid from the catalyst via **8**‡ and **9**‡ were also computed. Given the chemical similarities between these and state TS3, it is not surprising that the rate of this reaction step is also predicted to match the observed pK_a dependence.

4. Discussion

To argue that traditional β-hydride elimination through TS2 is the dominant mode of oxidation requires that reductive elimination of acetic acid through **8**‡ or **9**‡ determines the kinetics of the reaction, since TS2 cannot be responsible for the change in rate upon isotope or carboxylate substitution. Reaction through **9**‡ is unlikely, since its calculated activation enthalpy is significantly higher than that of TS3 and the measured activation enthalpy of 20.1 kcal/mol. Reaction through **8**‡ is thermodynamically feasible but is calculated to lead to a KIE of only 3.4 (Table 3).

The thermodynamics of benzyl alcohol oxidation (Figure 7) argue against the relevance of state **8**^{b‡}. **8**^{b‡} and **9**^{b‡} are thermodynamically even less favorable relative to TS3^{b‡} for this substrate than for 1-phenylethanol. Also, reaction of both substrates through **8**‡ cannot account for the disparate observed activation parameters (Figure 2). If a shift in resting state from **1** to **3**^{b} for benzyl alcohol is responsible for its higher activation entropy, the resulting calculated activation enthalpy ($\Delta H^{\ddagger}$(**3**^{b} → **8**^{b‡}) = 30.5 kcal/mol) would be inconsistent with the experimental measurement (likewise in the case of 2-decanol).

Finally, the recent observation of enantioselectivity in the oxidation of 1-phenylethanol in the presence of a C_2-symmetric carbene ligand[47] argues that reaction rates are influenced by an intermediate or transition state in which the chiral substrate is in intimate contact with the ligand. This confirms that the elimination of acetic acid (through either **8**‡, **9**‡, or **15**‡) does not determine reaction rates, if it influences them at all.

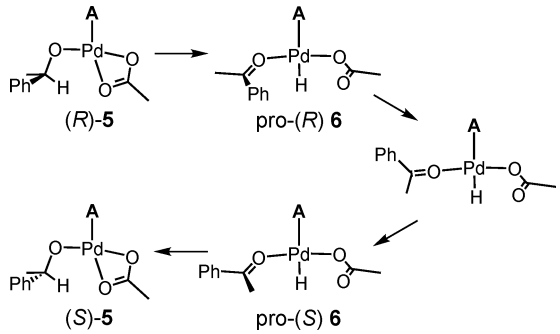

Figure 8. Possible mechanism of racemization.

Alternatively, one could argue that β-hydride elimination through TS1 is the major C−H bond scission pathway. However, this requires that the preceding liberation of acetic acid (**11**‡) is responsible for the observed activation enthalpy, while reductive elimination of the second acid unit (**15**‡) contributes the high KIE and dependence of rate on carboxylate. A rate law capable of satisfying these conditions has not been identified, much less one which also contains the required inverse dependence on acid concentration.

Thus, we conclude that oxidation by reductive β-hydride elimination (TS3) is the dominant mechanism of reaction. The theoretical description of this route is consistent with all experimental observations and yields a lower activation barrier than any other mechanism. Even if a negligible amount of substrate reacts through **8**‡ or **9**‡, it could still be that the system often passes through TS2 to state **6**, and then recrosses TS2 *unproductively*. Furthermore, we suspect that, in state **6**, rotation of the ketone (bound to palladium through oxygen) around the O=C bond axis would be facile (Figure 8). If this C−H activation and rotation were fast enough to equilibrate the *R* and *S* isomers of **5**, this catalyst could racemize an optically pure secondary alcohol independently of any simultaneous oxidation reaction. This process would undermine any attempt to perform a kinetic resolution using a chirally modified ligand. The occurrence of such a racemization could be determined experimentally by monitoring the oxidation of an enantiomerically pure substrate. If racemization is a reality for the catalyst formulation studied here, the relative rates of oxidation and racemization may still be tuned by variation of the carboxylate and ligand. Specifically, replacing acetate with pivalate has already been shown to simultaneously decrease the activation enthalpy associated with TS3 and increase that of TS2 (Table 4). The increased rate of oxidation of the pivalate-based catalyst was demonstrated in ref 8. The possibility of extending this

(46) Since the calculated dimerization energies of the carboxylic acids are independent of pK_a, the assumption that liberated acid exists as dimers in solution does not affect these relations.

(47) Mercer, G. J.; Sturdy, M.; Jensen, D. R.; Sigman, M. S. *Tetrahedron* **2005**, *61*, 6418.

effect by substituting tropolone ($pK_a = 6.7$[48]) for the carboxylic acid was investigated computationally. Thermodynamics employing a simplified carbene (1,3-dimethylimidazol-2-ylidene) on palladium ditropolonate suggested that reaction of 1-phenylethanol through either TS2 or TS3 would involve prohibitively high barriers ($\Delta H^{\ddagger} > 30$ kcal/mol). Also, the bulk of the carbene may affect the ability of the bound ketone to reorient. Although transition state TS2 has not been located using benzyl alcohol or 2-decanol, the relative enthalpies of TS3 and intermediate **6** for the various substsrates are not uniform. The possible competition between oxidation and racemization will therefore also be substrate dependent.

5. Conclusions

The reactivity of the $(NHC)Pd(OAc)_2$ complex **0** is distinguished from related palladium complexes of nitrogen-donor ligands by the strong trans influence of the carbene ligand. The formation of covalent bonds trans to the carbene is thermodynamically discouraged (cf. **13** and **6** or **2b** and **10**). Accordingly, the lowest-energy oxidation mechanism avoids forming a hydride in this position by shuttling the β-hydrogen of the substrate directly to the free oxygen of a metal-bound acetate group. The geometry and vibrational properties of this transition state lead to an unusually high kinetic isotope effect, and the predicted dependence of the rate of this reaction on isotope and carboxylate pK_a matches experiment. An alternative mechanism featuring traditional β-hydride elimination followed by reductive elimination of acetic acid lies slightly higher in energy, with the latter elementary step also in agreement with the experimental kinetic measurements. The potential energy surface suggests that reversible β-hydride elimination may enable the racemization of a chiral substrate. We recommend an experimental investigation of the racemization of an optically pure sample by these catalysts. This would shed light on the small energetic distinctions among the elementary steps of oxidation and possible racemization. These distinctions and their dependence on substrate and carboxylate (e.g., that more basic carboxylates will favor oxidation over racemization) will be critical in designing enantioselective catalysts.

Acknowledgment. We thank the group of Prof. Brian Stoltz at Caltech and Dr. Jonas Oxgaard for helpful discussions. This research was funded by the NSF (CTS-0548774) and by the Chevron-Texaco Energy Research and Technology Company. The facilities used for these studies were funded by grants from ARO-DURIP, ONR-DURIP, and NSF-MRI. All calculations were performed with Jaguar 5.0.[49]

Supporting Information Available: Thermodynamic properties and coordinates of numbered structures and vibrational frequencies of transition states. This material is available free of charge via the Internet at http://pubs.acs.org.

JA060915Z

(48) Breheret, E. F.; Martin, M. M. *J. Lumin.* **1978**, *17*, 49.
(49) *Jaguar 5.0*; Schrödinger, L.L.C., Portland, OR, 1991−2003.